Determination of total rock porosity from litho-density log data (example from the NEAT-borehole SB3-Tujetsch)

Autor(en): **Wyder, Renato Franco / Rybach, Ladislaus**

Objekttyp: **Article**

Zeitschrift: **Schweizerische mineralogische und petrographische Mitteilungen = Bulletin suisse de minéralogie et pétrographie**

Band (Jahr): **76 (1996)**

Heft 2

PDF erstellt am: **02.05.2024**

Persistenter Link: https://doi.org/10.5169/seals-57703

SCHWEIZ. MINERAL. PETROGR. MITT. 76, 277–296, 1996

Determination of total rock porosity from litho-density log data (example from the NEAT-borehole SB3-Tujetsch)

by *Renato Franco Wyder*[1] and *Ladislaus Rybach*[2]

Abstract

Two independent methods to determine total rock porosity from density logs are presented and compared. The first one estimates matrix densities from maximum log readings, the second uses repeated pyknometric measurements of rock matrix densities on 57 samples. The latter also enables error calculation and sensitivity analysis of porosity determination. The comparative use of both methods compensates to a certain degree the lack of knowledge about the absolute errors. The porosity results are substantiated by laboratory measurements. Although this work focuses mainly on methodology, it yielded the geologically interesting result that the northern Tavetsch massif exhibits high porosity even at depths exceeding 500 m.

Keywords: total porosity, matrix density, bulk density, logging, error analysis, kakirite, Tavetsch massif, Central Swiss Alps.

1. Introduction

The determination of total porosity from borehole logs (density, neutron, sonic) is a well established and routinely applied method to investigate sedimentary formations. Especially in hydrocarbon exploration the porosity profiles are indispensable ingredients of reservoir calculations. In the following, an application to crystalline rocks encountered in the NEAT ("Neue Eisenbahn-Alpen-Transversale")-borehole SB3-Tujetsch – i.e. gneisses and schists, partly kakiritized, of the Tavetsch massif, Swiss Alps – is presented, referring to problems in engineering geology (deep tunneling).

Although the basic principles of porosity determination from formation density logs (see chapter 2.1.) apply not only to sediments but also to crystalline rocks, no such study has been performed so far in deep drilling projects like Kola and KTB, Hot Dry Rock projects like Fenton Hill, Cornwall, Soultz or radwaste disposal studies like Nagra drillholes. To our knowledge only NELSON and JOHNSTON (1994) made explicitely an attempt, in a 125 m long granite section, to determine porosity from density logs. Also, only a few porosity determinations have been reported by combining different logs (BROGLIA and MOOS, 1988; ZIMMERMANN et al., 1992). The aim of this study is to evaluate the potential and limitations of porosity determination of crystalline rocks from density logs.

A sonic log was also run in borehole SB3. In principle, porosity determination would also be possible on the basis of the measured sonic Δt's. However, this kind of porosity determination calls for a detailed knowledge of matrix Δt's, which are generally not available for the crystalline rocks encountered in SB3. Thus the only feasible way to arrive at crystalline porosities is the density log approach.

During the years of 1991–1993, three investigation holes have been drilled in the northern Tavetsch massif by the drilling company FORALITH AG (Gossau/SG) in order to obtain information on the poorly exposed rocks of the Sedrun area (Fig. 1). In order to plan the construction of the roughly N–S oriented Gotthard base tunnel, the main goal of the boreholes has been the coverage of a horizontal section from the Vorderrhein to the southern part of the Aar massif. Because of the subvertical stratification of the rocks in the Tavetsch massif, the boreholes have been obliquely drilled with a dip of approximate-

[1] Mineralogisch-Petrographisches Institut, Universität Basel, Bernoullistr. 30, CH-4056 Basel, Switzerland.
[2] Institut für Geophysik ETHZ, ETH-Hönggerberg, CH-8093 Zürich, Switzerland.

ly 45°. The drilled rock profile covers a horizontal section length of about 1550 m. The total length of all boreholes is 2156.80 m. Single hole lengths are 833.50 m (SB1-Nord), 543.30 m (SB2-Süd) and 780.00 m (SB3-Tujetsch) respectively. None (!) of these holes reached the planned level of the base tunnel (approximately 560 m above sea level). The borehole bottoms are located 390 m (SB1-Nord), 550 m (SB2-Süd) and 300 m (SB3-Tujetsch) above the tunnel level. This work deals only with borehole SB3-Tujetsch.

1.1. GEOLOGICAL SETTING

The Tavetsch massif is a long and narrow geological body and tectonic unit between Aar- and Gotthard massif consisting of subvertical bedded rocks, pendling around north- and southward dipping, and following the regional east–west striking trend (Fig. 1). With a mean width of 2.5 km and a maximum width of 5 km the Tavetsch massif is present from east of Andermatt (Oberalp Pass area) to the area east of Schlans. Southward, the Urseren-Garvera-sedimentary zone separates the Tavetsch massif from the Gotthard massif. In the north, the transition into the Aar massif is not unambiguous everywhere. East of Disentis, the sedimentary Disentis zone separates the two massifs. But westwards in the Sedrun area clearly sedimentary separating outcrops are lacking. The units are distinguished on the basis of structural and petrographic features, e.g. the decrease of biotite occurrence within the Tavetsch massif, the general reduction in grain size and the stronger foliation compared to rocks of the Aar massif. In addition, large kakiritic shear zones (ten to twenty meter range) with intermingled rocks of both massifs build up the transition into the Aar massif. With reference to the drillsites SB1-Nord and SB2-Süd these shear zones are summarized as "Clavaniev zone" (SCHNEIDER, 1991).

NIGGLI (1944) subdivides the rocks of the Tavetsch massif into seven groups: a) paragneiss-

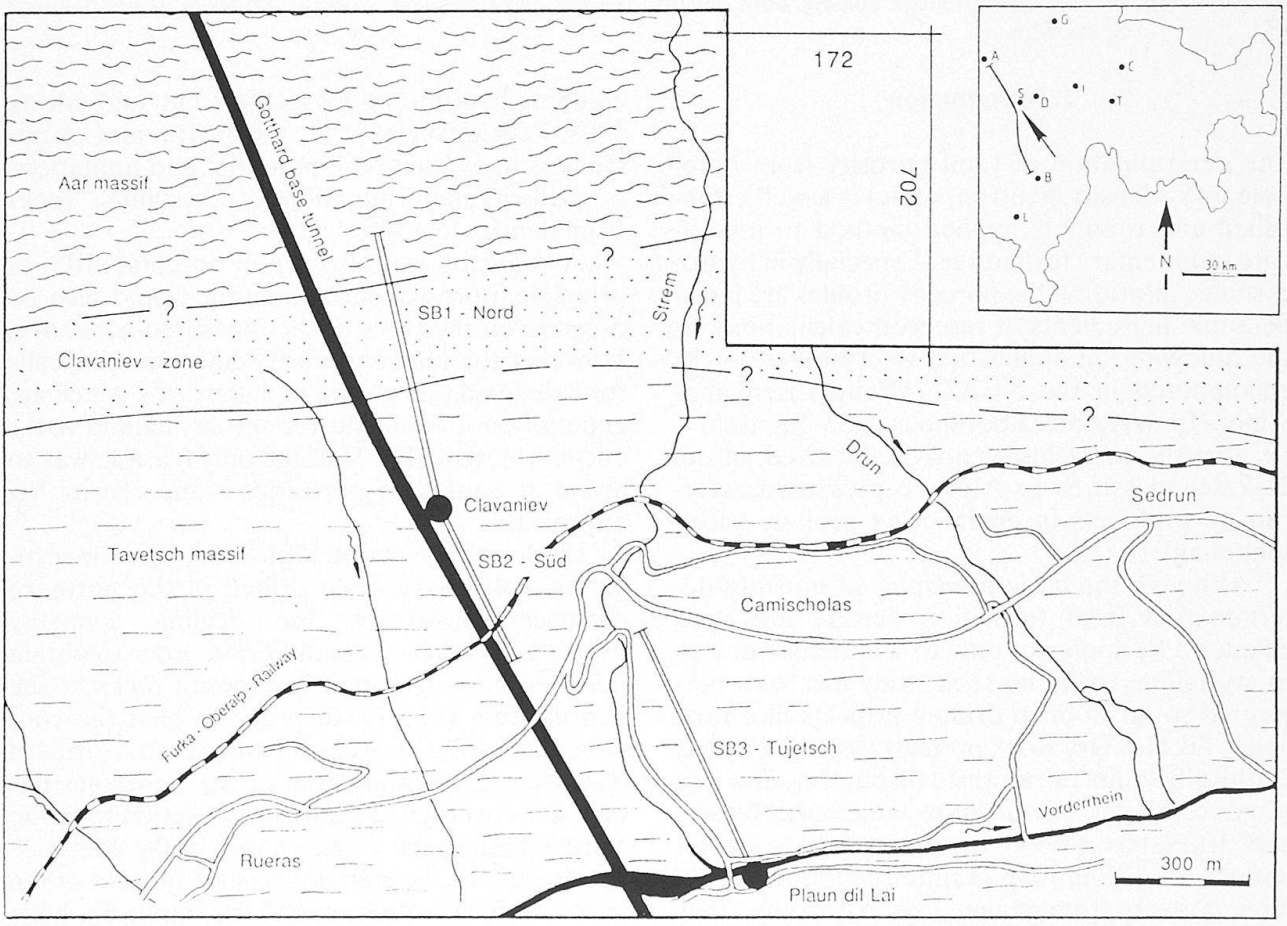

Fig. 1 Simplified map with the locations and traces of the three NEAT boreholes. This work only deals with SB3-Tujetsch. Bold line = trace of the planned Gotthard base tunnel. Inset: A = Andermatt, B = Biasca, C = Chur, D = Disentis, G = Glarus, I = Ilanz, L = Locarno, S = Sedrun, T = Thusis. Coordinates correspond to the 1 km grid of the "Schweizerische Landeskarte 1:25'000".

es (including rocks of hornfels character), b) paraschists (with quartzites), c) injection- and mixed gneisses, d) amphibolites and greenschists, e) ultrabasites, f) quartz porphyries (including felsic, turmaline bearing types), g) pegmatite dykes and (sometimes ore bearing) quartz dykes.

In the drilled profile of SB3-Tujetsch, most of the rocks belong to the groups a) and b) with some intercalations of groups c) and d). In addition, some aplitic formations, occur that are nowhere visible on the surface.

The Tavetsch massif marks the eastern part of the Rhine–Rhone suture line and is highly affected by ductile and brittle tectonic deformation. There is a noteworth decrease in rigidity and cohesion of the rocks compared to the rocks of the Aar- and Gotthard massif. Cohesionless kakirites (HEITZMANN, 1985) are very common and have been described first by NIGGLI (1944) in this area. Because most of the massif is covered by thick Quaternary sediments, outcrops are rare and only sparse information can be obtained from them. In addition, the low strength rocks of the Tavetsch massif show very limited resistance against surface processes like weathering, erosion or tipping downslope.

1.2. THE BOREHOLE SB3-TUJETSCH

From the location Plaun dil Lai (Coordinates: 700 : 900/170 : 925, Fig. 1) near the entrance to the gallery of the power station Vorderrhein the borehole SB3-Tujetsch was drilled 780 m downwards with a mean dip of 50° and a mean azimuth of 338°. It reached a depth of 480 m below surface. Drilling work started on August 10th, 1993 and ended on November 30th, 1993.

The most important result is that 30% of the borehole length consists of cohesionless rocks, so-called kakirites. The rest of the drilled profile is composed of very soft, brittle and only rarely solid rocks. From visual inspection of core samples a generally high porosity of these rocks becomes obvious. Because only less than 3.5% of the core samples in the drilled profile have been lost during extraction, the derivation of the 30% fraction of cohesionless material in the borehole has been made possible by applying accurate "rock-statistics" (= abundance of rock types in the drilled section in %, derived from visual observation: SCHNEIDER, 1993). These statistics describe the lithological and textural variations of the rocks along the drilled profile (gneiss, gneiss to schist, schist, phyllite) as well as the distribution and abundance of kakirites within given textural rock types (% length). To enable the identification of larger-scale lithologic trends as well as for drillsite forecasts, the statistics comprise 50 m intervals. The smallest registered length within the statistic data is 1 cm.

1.3. OBSERVATIONS DURING LOGGING

On October 24/25, 1993 and December 01/02, 1993 the company SCHLUMBERGER (Hannover/D) acquired geophysical well logs in the depth range between 299 m and 780 m of SB3-Tujetsch:

– FMS (Formation Microscanner), CAL (Caliber) and SGR (Natural Gamma Ray sum-curve): Measurement of rock structures and borehole deviation (FMS), borehole diameter (CAL) and depth reference (SGR).

– DLL (Dual-Laterolog) including SP (Spontaneous Potential): Measurement of electrical resistivity. Indicator for porosity and lithology. SP values are not usable because of interferences with the nearby electric power station.

– NGT (Natural Gamma Ray Spectrometry): Indicator for mineralogical changes. Measurement of thorium, uranium and potassium.

– AS (Array Sonic) including SGR: Registration of p- and s-wave velocities. Indicator for dynamic elastic modulus (mechanical properties).

– HLDL (High Resolution Litho–Density Log): Registration of photoelectric factor (PEF) and rock density. Indicator for lithology and porosity.

– TEMP: Measurement of Bottom Hole Temperature (BHT) during all runs.

The evaluation of the log data revealed that, in large parts, the rock densities lie below reasonable values for the rock types encountered in the borehole. At the same time the borehole diameter (CAL) remained fairly stable and the borehole compensation of the density log was working correct at any time (DRHO trace). Larger breakouts occur in the ranges 310 m – 330 m and 536 m – 548 m only. Both ranges marked the beginnings of the open borehole during the log campaigns. For the first range density measurements on small rock cubes proved, that the borehole diameter has no influence on the density values. For the second range the breakout influence is believed to be small, although no comparing density measurements on rock cubes could be performed.

Many density values in SB3 lie below the density of pure quartz (2.65 g/cm^3) and thus indicate high porosity. On the other hand, packer tests done by SOLEXPERTS AG (Schwerzenbach/ZH) in the depth ranges 537.80 m – 552.00 m and 760.00 m – 780.00 m with corresponding investigation depth intervals between 5.9 to 10 m, indi-

cate very low transmissivity values (between 1 and 7.7 · 10^{-8} m^2/s) and values of hydraulic conductivity (= k, between 9.1 · 10^{-10} up to 5.4 · 10^{-9} m/s) (SCHNEIDER, 1994). Both packer tests have been performed within rock sections that are highly affected by brittle deformation and exhibit pure kakiritic length portions of around 30% and 40% respectively.

1.4. INCENTIVES OF STUDY

The combination of high porosities and low permeability stimulated this detailed porosity study, on the basis of the available density logs. The aim was to calculate two porosity profiles by applying two independent methods of porosity determination. The first method is an empirical estimation, whereas the second one includes pyknometric measurements of rock matrix densities. In addition, the second method includes error analysis based on error propagation, considering the mean errors of the measured parameters. This analysis can identify error-sensitive parameters (chapter 4); in addition it enables a more exact definition of such parameters and thus provides means to reduce the error of the final (porosity) result.

1.5. DEFINITIONS, CONVENTIONS, SYMBOLS

In general terms, porosity gives the volume fraction of rock that is not occupied by solid (mineral) constituents. The pore space can be filled with fluids and/or gas. Different types of porosity can be distinguished (SERRA, 1984):

– total porosity Φ_t: total volume fraction of a rock not taken by solids;

– interconnected porosity Φ_i: fraction of Φ_t which is in communication;

– potential porosity Φ_p: fraction of Φ_i with large enough spaces to enable fluid movement (pore diameter > 50 μm for oil, + 5 μm for gas);

– effective (usable) porosity Φ_e: fraction of Φ_p available for fluid passage, i.e. excluding e.g. the volume occupied by water adsorbed on clay minerals.

In this study, porosity Φ always refers to total porosity (Φ_t). Φ is related to the bulk density ρ_b of the rock, which is the quantity computed from ρ_e, the value measured by the litho-density logging tool (see chapter 2):

$$\Phi = \frac{(\rho_{ma} - \rho_b)}{(\rho_{ma} - \rho_{fl})} \qquad (1)$$

where ρ_{ma} denotes the density of the rock matrix and ρ_{fl} the density of the pore filling. ρ_{ma} is the rock density for $\Phi = 0$.

Tab. 1 Abbreviations and symbols.

Mathematical symbol	Log evaluation symbol in computing	Meaning in log evaluation	Geological meaning
ρ_{ma}	RHOMA	Matrix density	Grain density
ρ_b	RHOB	Bulk density	Rock density
ρ_{fl}	RHOFL	Fluid density	Pore fluid density
Φ	PHI	Porosity	Total porosity
$\Delta\Phi$	ΔPHI	Mean error of porosity	Mean error of porosity

During log evaluation the term "matrix" refers to all solid constituents of a rock (mineral grains, matrix in the sense of sedimentology, cement keeping the grains together). Pore filling (= "fluid") may be water, brine, air, hydrocarbons etc.).

In matrix density (ρ_{ma}) determinations, four significant digits behind the decimal point were used. Log readings (ρ_b) are given with three digits, fluid densities (ρ_{fl}, measured on drilling muds by hydrostatic balance) with two digits. All calculations have been performed up to four digits and rounded afterwards to two digits. Porosities are given in volume %, all densities in g/cm^3. Table 1 lists all abbreviations/symbols used in the numerical calculations.

2. Methodology

2.1. LOGGING PRINCIPLE

The litho-density equipment measures scattered gamma radiation of an isotopic source (mostly ^{137}Cs) at a fixed distance (L, spacing). The interaction of the emitted gamma rays with atoms of the rock formation surrounding the borehole depends on the energy level of the gammas (in MeV): a) at low energies (< 0.1 MeV) the photoelectric effect dominates, b) at intermediate levels (0.1–2 MeV) the interaction is predominantly by Compton scattering, and c) above 2 MeV the interaction is by electron-positron pair production.

Because the most commonly used ^{137}Cs source emits monoenergetic gamma quanta with 0.66 MeV, only Compton scattering must be considered in logging practice. In this case, the scatterers are electrons and the interaction can be described as

$$\Psi = \Psi_i \exp(-\rho_e \sigma h) \qquad (2)$$

where Ψ_i is the incident photon (gamma) flux, h the scatterer (here rock) thickness (≈ L), σ the Compton cross section, ρ_e the electron density

(= number of electrons per unit volume), and Ψ the photon flux leaving the scatterer (to be measured). For electrons in a material of mass density RHOB,

$$\rho_e = (Z/A)N_A \rho_b \quad (3)$$

where Z is material atomic number, A material atomic weight, and N_A Avogadro's number (= $6.02 \cdot 10^{23}$). Since the ratio Z/A for most elements encountered in logging is fairly constant (= 0.50), ρ_e (to which the litho-density log reacts) is directly proportional to RHOB, in sedimentary as well as in crystalline rocks.

In practice, the gamma quanta emitted by the source diffuse through the rock formation and loose energy through Compton scattering. At a fixed distance from the source (L), when a low-electron density material is present, there is a high-detector count rate of remaining backscattered gamma rays. With high electron density material there is a low-detector count rate, and a greater statistical count rate variation. Scintillation detectors with NaI crystals are most common to record the backscattered gammas, which originate from the immediate surroundigs of the borehole. Two detectors at different spacings are frequently used in order to compensate for borehole effects. Source and detectors are mounted on a skid, sliding along the borehole wall. The logs display already the corrected bulk density RHOB. For a more detailed discussion see e.g. DESBRANDES (1985) or ELLIS (1987).

2.2. PROCEDURE APPLIED

The bulk density values (RHOB) are read from the measured logs. To calculate PHI, reliable values of RHOMA are needed only, cf. equ. (1), since RHOFL is given by daily measurements on the drillsite. In particular, two different methods were used to estimate the porosity profile of the investigated borehole profile:

1) The logged profile is subdivided into a number (in our case 35) of lithologic zones with uniform matrix density; the highest RHOB value of the zone is assigned to the entire zone as matrix density (= RHOMA (1)).

2) To obtain estimates of the matrix density along the entire investigated borehole and by using lithologic criteria 57 RHOMA values from pyknometer determinations of selected samples (= RHOMA (2)) were assigned to those portions of the profile, which contained the individual sample points within a maximum distance of 14 m. This yields a geologically more realistic density distribution than the RHOMA (1)-method.

Both methods are mentioned in SERRA (1984) and TITTMAN (1986). In case of the second approach the mean error of the RHOMA values is also known (Tab. 2) and an error calculation can be performed (chapter 4).

2.3. THE DETERMINATION OF MATRIX DENSITIES (RHOMA)

Values of RHOMA (1) lead to calculated porosities PHI (1) whereas RHOMA (2) yields porosities PHI (2), and error values ± ΔPHI (2).

2.3.1. First method: division of the logged profile in zones of constant matrix densities and estimation of RHOMA (1)

In general, the mineralogical composition in SB3 is a combination of six main constituents. Ordered by increasing densities these are albite (2.62 g/cm³), quartz (2.65 g/cm³), calcite (2.71 g/cm³), chlorite (2.77 g/cm³), muscovite (2.83 g/cm³) and biotite (3.01 g/cm³). Although opaque minerals may form single layers occasionally, they make up less than 5% of the rock volume. In most cases, the opaque mineral is pyrite (5.00 g/cm³).

Theoretically the lowest density for the rock matrix would be 2.62 g/cm³. This corresponds to a monomineralic albite rock. The upper end member (without opaque minerals) would be a rock consisting of biotite only with a density of 3.01 g/cm³. As a first approximation of RHOMA (1) it can be said that rocks with a density below 2.62 g/cm³ *must* be porous, whereas rocks with a density higher than 3.01 g/cm³ *can* be porous but *must* contain opaque minerals.

Because of the mineralogical and lithological heterogeneity of the rocks the drilled profile must be divided into zones of constant matrix density leading to 5 categories with RHOB < 2.5 g/cm³, 2.5 < RHOB < 2.6 g/cm³, 2.6 < RHOB < 2.7 g/cm³, 2.7 < RHOB < 2.8 g/cm³ and RHOB > 2.8 g/cm³.

Based on several criteria, 35 zones have been distinguished (Tab. 2). For example zone 8: Most RHOB values lie between 2.7 g/cm³ and 2.8 g/cm³ and the maximum RHOB value is 2.813 g/cm³ (= RHOMA (1) for zone 8). In addition, the mineralogical composition is fairly constant and the log traces show tendencies that are significantly different from zone 7 and zone 9. The density subdivision should be in agreement with other logging data as seismic velocities, photoelectric factor, electrical resistivity and natural Gamma ray spectrometry. Care must be taken in interpreting changes in log trace tendencies. Since seismic velocities, electrical resistivities and photoelectric

Tab. 2 Method 1: The subdivision of the logged profile in zones and estimated matrix densities. Due to the borehole inclination the colums "from" and "to" do not correspond to vertical depth. "Blank" intervals contain no data. They mark the distance between the log read position defining the end of a zone and the log read position defining the beginning of the next zone. Method 2: Pyknometric measurements of RHOMA (2), depth corresponding values RHOMA (1), and the corresponding calculated values of PHI (1) and PHI (2). All values of RHOMA (2) are mean values of pyknometer measurements. RHOFL is 1.05 g/cm³ in the depth range 299 m – 535 m and 1.03 g/cm³ from there on. ΔRHOB is ± 0.01 g/cm³. Correlation: Ratios of matrix densities and corresponding porosities. Values of 1.00 indicate perfect agreements between method 1 and 2.

Method 1							Method 2							Correlation	
Zone	from (m)	to (m)	Interval (m)	Blank (m)	Σ(Int. + Blank) (m)	RHOMA (1) (g/cm³)	Sample depth (m)	RHOB (g/cm³)	RHOMA (2) (g/cm³)	±ΔRHOMA (2) (g/cm³)	PHI (1) (%)	PHI (2) (%)	±ΔPHI (2) (% of PHI)	RHOMA (1)/ RHOMA (2)	PHI (1)/ PHI (2)
0 (Casing)	299.00	300.90	1.90	0.10	2.00	2.696									
1	301.00	308.50	7.50	0.10	7.60	2.742	305	2.6390	2.8138	0.0052	6.09	9.91	6.32	0.97	0.61
2	308.60	314.00	5.40	0.10	5.50	2.742	312	2.7020	2.8074	0.0030	2.36	6.00	9.86	0.98	0.39
3	314.10	331.30	17.20	0.10	17.30	2.742	322	2.6370	2.8093	0.0012	6.21	9.79	5.84	0.98	0.63
							325	2.6310	2.8042	0.0041	6.56	9.87	6.16	0.98	0.66
							329	2.5310	2.7533	0.0022	12.47	13.05	4.58	1.00	0.96
							330	2.6080	2.8279	0.0043	7.92	12.37	4.86	0.97	0.64
							331	2.6290	2.8120	0.0066	6.68	10.39	6.35	0.98	0.64
4	331.40	356.40	25.00	0.10	25.10	2.812	334	2.7060	2.8017	0.0022	6.02	5.46	10.67	1.00	1.10
							348	2.7590	2.7952	0.0017	3.01	2.07	28.00	1.01	1.45
5	356.50	361.30	4.80	0.10	4.90	2.770	360	2.5980	2.8085	0.0013	10.00	11.97	4.78	0.99	0.84
6	361.40	374.30	12.90	0.10	13.00	2.770	364	2.6660	2.7662	0.0026	6.05	5.84	10.27	1.00	1.04
							370	2.6790	2.8029	0.0027	5.29	7.07	8.32	0.99	0.75
7	374.40	378.50	4.10	0.10	4.20	2.770	375	2.6920	2.8577	0.0007	4.53	9.17	6.05	0.97	0.49
							378	2.5300	2.7663	0.0022	13.95	13.77	4.31	1.00	1.01
8	378.60	399.30	20.70	0.10	20.80	2.813	385	2.6830	2.8058	0.0008	7.37	6.99	8.17	1.00	1.05
							394	2.7610	2.7752	0.0004	2.95	0.82	70.48	1.01	3.58
9	399.40	439.30	39.90	0.10	40.00	2.781	405	2.6880	2.7594	0.0027	5.37	4.18	14.47	1.01	1.29
							408	2.5820	2.8621	0.0013	11.50	15.46	3.59	0.97	0.74
10	439.40	452.30	12.90	0.10	13.00	2.790/ 3.289	440	2.7550	2.7387	0.0016	2.01	–0.97	62.15	1.02	–2.08
							450	2.6940	2.8008	0.0030	5.52	6.10	9.73	1.00	0.90
11	452.40	477.10	24.70	0.10	24.80	2.729	462	2.6760	2.7407	0.0008	3.16	3.83	15.50	1.00	0.82
12	477.20	492.50	15.30	0.10	15.40	2.736	480	2.7350	2.7580	0.0027	0.06	1.35	44.99	0.99	0.04
							482	2.6320	2.7621	0.0022	6.17	7.60	7.84	0.99	0.81
13	492.60	495.80	3.20	0.10	3.30	2.858	495	2.8110	2.8912	0.0058	2.60	4.36	14.26	0.99	0.60
14	495.90	512.60	16.70	0.10	16.80	2.699	510	2.5880	2.7275	0.0054	6.73	8.32	8.00	0.99	0.81
15	512.70	514.10	1.40	0.10	1.50	2.789	513	2.7650	2.7697	0.0026	1.38	0.27	219.80	1.01	5.05
16	514.20	528.40	14.20	0.10	14.30	2.694	519	2.5980	2.8131	0.0012	5.84	12.20	4.67	0.96	0.48
							525	2.6300	2.7671	0.0006	3.89	7.98	7.31	0.97	0.49
17	528.50	548.49	19.99	0.15	20.14	2.630	536	2.5000	2.7610	0.0027	8.12	15.08	3.93	0.95	0.54
							545	2.5100	2.7775	0.0017	7.50	15.31	3.78	0.95	0.49

Tab. 2 (cont.)

18	548.64	561.29	12.65	0.15	12.80	2.730	553	2.6500	2.7645	0.0017	4.71	6.60	8.84	0.99	0.71
							556	2.6200	2.7399	0.0045	6.47	7.01	9.04	1.00	0.92
19	561.44	580.95	19.51	0.15	19.66	2.730									
20	581.10	594.82	13.72	0.15	13.87	2.690	586	2.6000	2.7547	0.0004	5.42	8.97	6.47	0.98	0.60
21	594.97	618.59	23.62	0.15	23.77	2.750	600	2.6900	2.7840	0.0025	3.49	5.36	10.93	0.99	0.65
							605	2.6700	2.8071	0.0028	4.65	7.71	7.53	0.98	0.60
22	618.74	637.03	18.29	0.15	18.44	2.800	631	2.6700	2.8029	0.0037	7.34	7.50	7.95	1.00	0.98
							637	2.7000	2.7999	0.0026	5.65	5.64	10.31	1.00	1.00
23	637.18	650.14	12.96	0.15	13.11	2.730	639	2.6900	2.7368	0.0021	2.35	2.74	21.81	1.00	0.86
							645	2.6500	2.7974	0.0017	4.71	8.34	6.87	0.98	0.56
							647	2.6100	2.7374	0.0063	7.06	7.46	9.09	1.00	0.95
							648	2.6000	2.7187	0.0004	7.65	7.03	8.69	1.00	1.09
24	650.29	652.42	2.13	0.16	2.29	2.730	651	2.7000	2.7803	0.0073	1.76	4.59	15.15	0.98	0.38
25	652.58	668.88	16.30	0.16	16.46	2.820									
26	669.04	673.46	4.42	0.15	4.57	2.820	671	2.5300	2.7457	0.0055	16.20	12.57	5.14	1.03	1.29
27	673.61	679.86	6.25	0.15	6.40	2.700	676	2.6400	2.7271	0.0008	3.59	5.13	11.51	0.99	0.70
28	680.01	705.61	25.60	0.15	25.75	2.810	685	2.6300	2.7157	0.0017	10.11	5.08	11.82	1.03	1.99
29	705.76	714.91	9.15	0.15	9.30	2.710	707	2.6500	2.7585	0.0028	3.57	6.28	9.53	0.98	0.57
							710	2.5900	2.8616	0.0034	7.14	14.83	3.83	0.95	0.48
							714	2.6400	2.7045	0.0024	4.17	3.85	15.91	1.00	1.08
30	715.06	721.00	5.94	0.16	6.10	2.730	717	2.6800	2.7636	0.0037	2.94	4.82	12.68	0.99	0.61
							720	2.7100	2.7947	0.0027	1.18	4.80	12.19	0.98	0.25
31	721.16	729.39	8.23	0.15	8.38	2.760	725	2.7100	2.8359	0.0040	2.89	6.97	8.47	0.97	0.41
32	729.54	746.00	16.46	0.15	16.61	2.670	740	2.5700	2.8232	0.0050	6.10	14.12	4.30	0.95	0.43
							745	2.6200	2.8114	0.0044	3.05	10.74	5.61	0.95	0.28
33	746.15	747.22	1.07	0.15	1.22	2.730									
34	747.37	778.15	30.78	0.00	30.78	2.730	751	2.5500	2.7921	0.0052	10.59	13.74	4.62	0.98	0.77
							753	2.5300	2.7559	0.0038	11.76	13.09	4.66	0.99	0.90
							770	2.5800	2.7609	0.0043	8.82	10.45	5.92	0.99	0.84
							775	2.6400	2.7887	0.0024	5.29	8.46	6.89	0.98	0.63
	778.15	780.00	1.85		1.85										
	log-length		481.00				Min.	2.5000	2.7045	0.0004	0.06	–0.97	3.59	0.95	–2.08
							Max.	2.8110	2.8912	0.0073	16.20	15.46	219.80	1.03	5.05
							Mean	2.6445	2.7824	0.0029	5.89	7.89	15.10	0.99	0.83
							Median	2.6400	2.7803	0.0026	5.65	7.46	8.17	0.99	0.71

factor are strongly dependent of rock structures and mechanical behaviour, one must be sure, that changes are in agreement with lithological changes.

Zone 0 is a special case because half of the profile still lies within casings. To avoid effects of the casing steel, zone 0 contains the first meter of the open borehole. Another problematic case is zone 10. The presence of a predominant, discrete ore layer calls for two matrix densities in this zone.

After evaluating all the 35 zones, matrix densities are defined as the maximum densities measured by the logging tool in each zone. This means that every zone contains a porosity maximum and a porosity minimum (= 0%). The next step is to control RHOMA (1) in every zone, using the lithological profile. In our case it became obvious that because of lithological reasons the matrix densities of different zones are identical. In these corresponding zones the mineralogical contents on a mesoscopic scale are equal, but significant differences in RHOB, seismic velocities and electrical resistivities called for their separation during log analysis.

2.3.2. Second method: pyknometric measurements of RHOMA (2) and lithologic assignment over the logged profile

Pyknometric measurements of matrix densities (RHOMA (2) have been made on 57 core samples (Tab. 2) by applying the method described by MÜLLER (1964). 10 g of substance were used in a 50 ml pyknometer. The sample must be powdered in order to obtain matrix densities. It is essential that the grain size lies in a range where no pores are present in the single grains. Most of the samples used are so brittle and soft, that they could be desaggregated by hand. Further treatment included grinding and milling.

A 1:10 mixture of ethanol and water has been used to moisten the powdery probe. Finally an ultrasonic treatment for several minutes helped in evacuating as much air as possible from the powder in the pyknometer.

As the pyknometer is a very accurate tool, densities can be reproduced in the range of some thousandths down to some tenthousandths g/cm^3. In order to derive a standard deviation and a mean error for RHOMA (2), every sample has been measured at least three times.

The values of RHOMA (2) are then assigned as estimates to appropriate positions along the logged profile. Mesoscopically identical rocks obtain the same matrix densities. The maximum length of constant matrix density is 14 m and covers a thick monotonous formation. For the assignment of RHOMA (2) values the geological profile has been used (and not the log record).

The advantage of this method compared to the first one is better control of intercalated formations. Therefore the assignment of measured matrix densities RHOMA (2) is geologically more realistic than the distribution of maximum RHOB values for RHOMA (1).

2.3.3. Comparison between RHOMA (1) and RHOMA (2)

It is obvious that RHOMA (1) lies quite close to RHOMA (2). The ratios RHOMA (1) / RHOMA (2) are scattering between 0.95 and 1.03 (Tab. 2). The ratios PHI (1) / PHI (2), on the other hand, are scattering between –2.08 and 5.05 (Tab. 2). One suspects that the influence of wrong matrix densities on the resulting porosity is dramatic.

The negative PHI (2) value in table 2 (a single case) is the result of a poor pyknometer measurement. The matrix density was falling below the corresponding value of RHOB. In the calculation this leads to a negative and therefore unrealistic porosity. It is likely that the high content of fine grained sheet silicates in this sample prevented the complete air evacuation and moistening of the powder. In order to show the consequences concerning errors in the calculation of porosity profiles, this value remains in the data set and is assigned to the profile, however.

	all values (N = 3899)					realistic values (N = 3613)				
	RHOB (g/cm^3)	PHI (1) (Vol.%)	PHI (2) (Vol %)	PHI (1)/ PHI (2)	RHOMA (1)/ RHOMA (2)	RHOB (g/cm^3)	PHI (1) (Vol.%)	PHI (2) (Vol.%)	PHI (1)/ PHI (2)	RHOMA (1)/ RHOMA (2)
Min.	1.8700	0	–5.59	–45.26	0.95	2.4300	0	0	0	0.95
Max.	3.2890	50.59	51.57	130.38	1.03	3.2890	16.66	19.89	130.38	1.03
Mean	2.6501	6.05	7.28	1.08	0.99	2.6588	5.49	6.90	1.34	0.99
Med.	2.6700	5.14	6.17	0.8	0.99	2.6700	5.14	6.15	0.8	0.99

Tab. 3 Correlation between PHI (1) and PHI (2), including (left side) and ignoring (right side) the unrealistic values of PHI (2).

3. Calculation

Porosities are calculated according to equation (1). A total of 3899 porosity values has been calculated with RHOMA (1) as well as with RHOMA (2). The corresponding results are given in the Appendix "Por Listing" as PHI (1) and PHI (2). Figure 2 shows PHI (1) and PHI (2) plotted against depth. In figure 3 a small scale correlation over 25 m with the lithologic profile is shown.

3.1. POROSITY RESULTS

The depth range 570–580 m exhibits the highest porosity values (maximum > 50%). Here bulk densities are below 1.9 g/cm^3. This is far below realistic values for crystalline rocks, in this case a sericite-chlorite-feldspar-schist. Although the rock is soft and highly fractured (core observation and interpretation of the FMS image), one would not expect such high porosity values. The explanation lies in the cementation of the borehole. Because of the weak rock cohesion, the borehole had to be stabilized prior to logging by cement in the depth range between 556 m and 580 m. In the Appendix "Por Listing" all these values are collectively classified as unrealistic and shaded in grey colour.

Both porosity profiles correlate well (Fig. 2), as the curve shapes are quite similar. The main difference between the profiles is the occurrence of negative PHI (2) values. Two sources of error are leading to these values. Firstly, the poor pyknometric measurement of RHOMA (2) at 440 m yielding a negative porosity, secondly, bad guesses in the assignment of RHOMA (2). The first error is an analytical one, whereas the second has geological reasons. All negative values of PHI (2) are classified as unrealistic. Including the cemented part of the borehole (158 values), there are 286 unrealistic values (of a total of 3899).

In the PHI (1) profile the assignment of matrix densities as maximum interval densities prevents the occurrence of negative results. The only geologically unrealistic values are those in the cemented region.

In order to better correlate PHI (1) and PHI (2), table 3 correlates the statistics between all values (3899) and realistic values (3613).

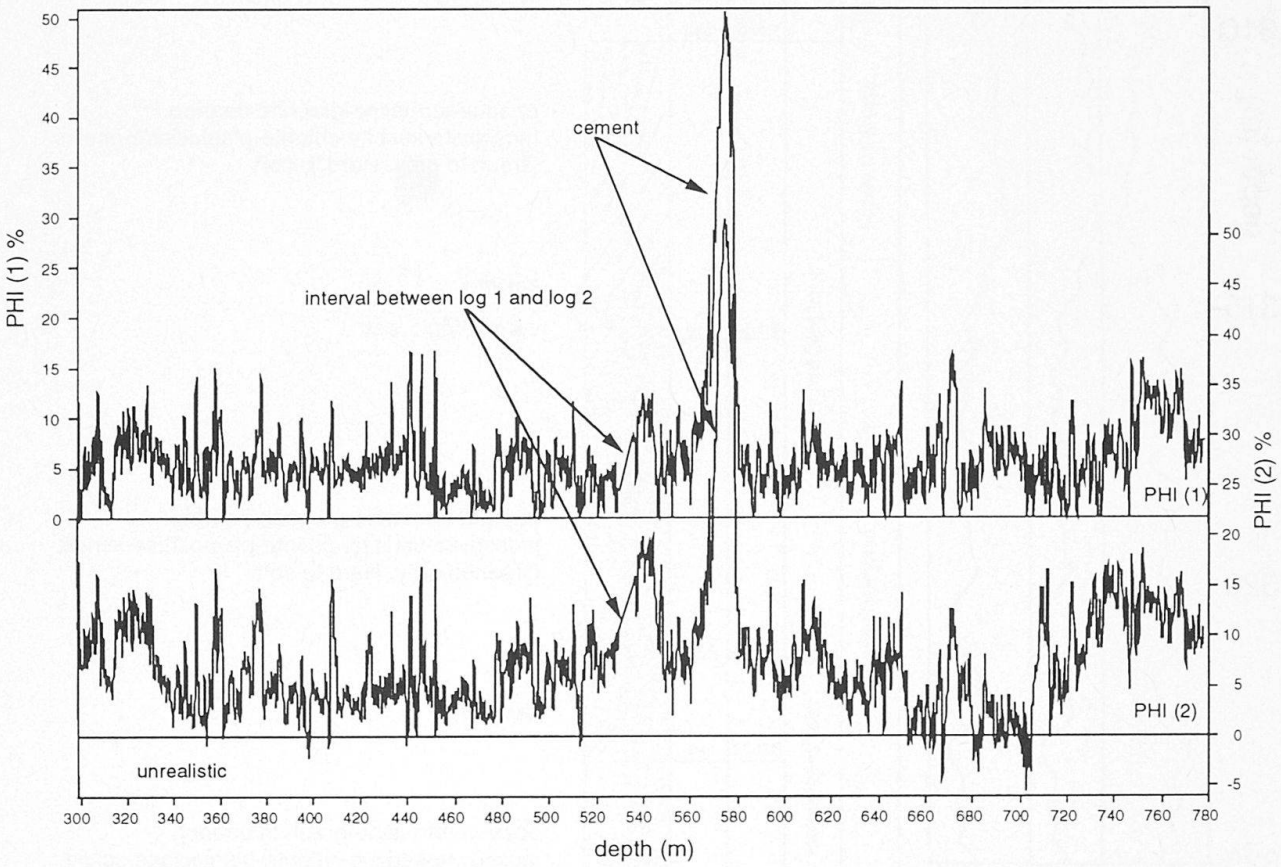

Fig. 2 Upper curve: porosity profile calculated with method 1; unrealistic values in the cemented section. Lower curve: porosity profile calculated with method 2; unrealistic values in the cemented section. Negative (unrealistic) values correspond to a poor pyknometric measurement at 440 m, as well as to bad guesses in the assignment of RHOMA (2).

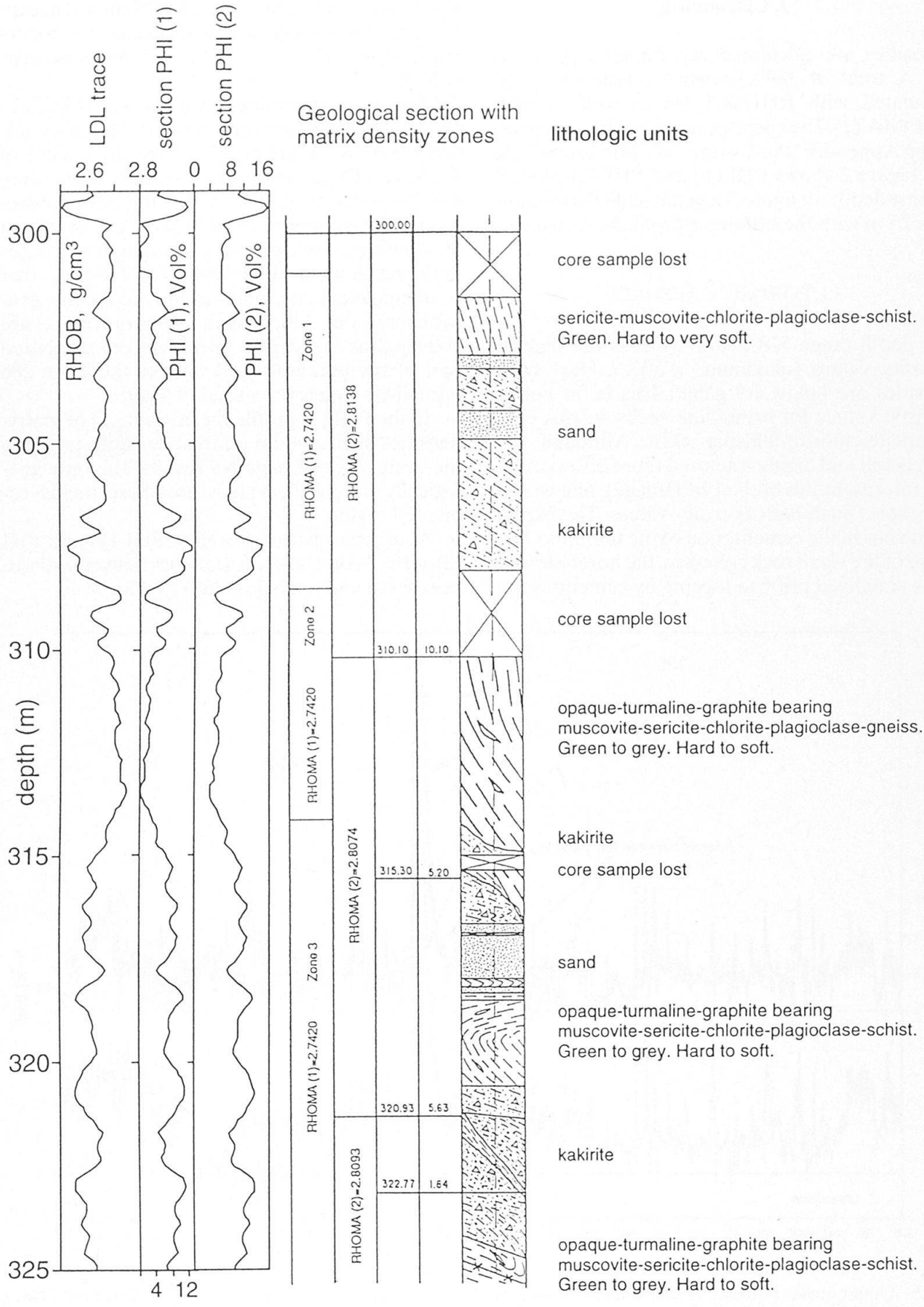

Fig. 3 Small scale correlation between RHOB, PHI (1), PHI (2) and the geological section. The accuracy of the depth position of core samples decreases with increasing depth, therefore correlations must be done with much care, and by consulting other log traces (e.g. FMS-image).

Except for the minimum value of PHI (2) the porosities PHI (2) are generally higher than the porosities PHI (1). This is well expressed in the profiles (Figs 2 and 3) and also in statistical diagrams (Fig. 4). The interpretation that maximum values of RHOB do not correspond to zero-porosity seems reasonable, i.e. the maximum density values in such zones still correspond to porosities > 0%. In the profile PHI (1) the values in the cemented borehole part are classified as unrealistic, as well as the negative values in the profile PHI (2).

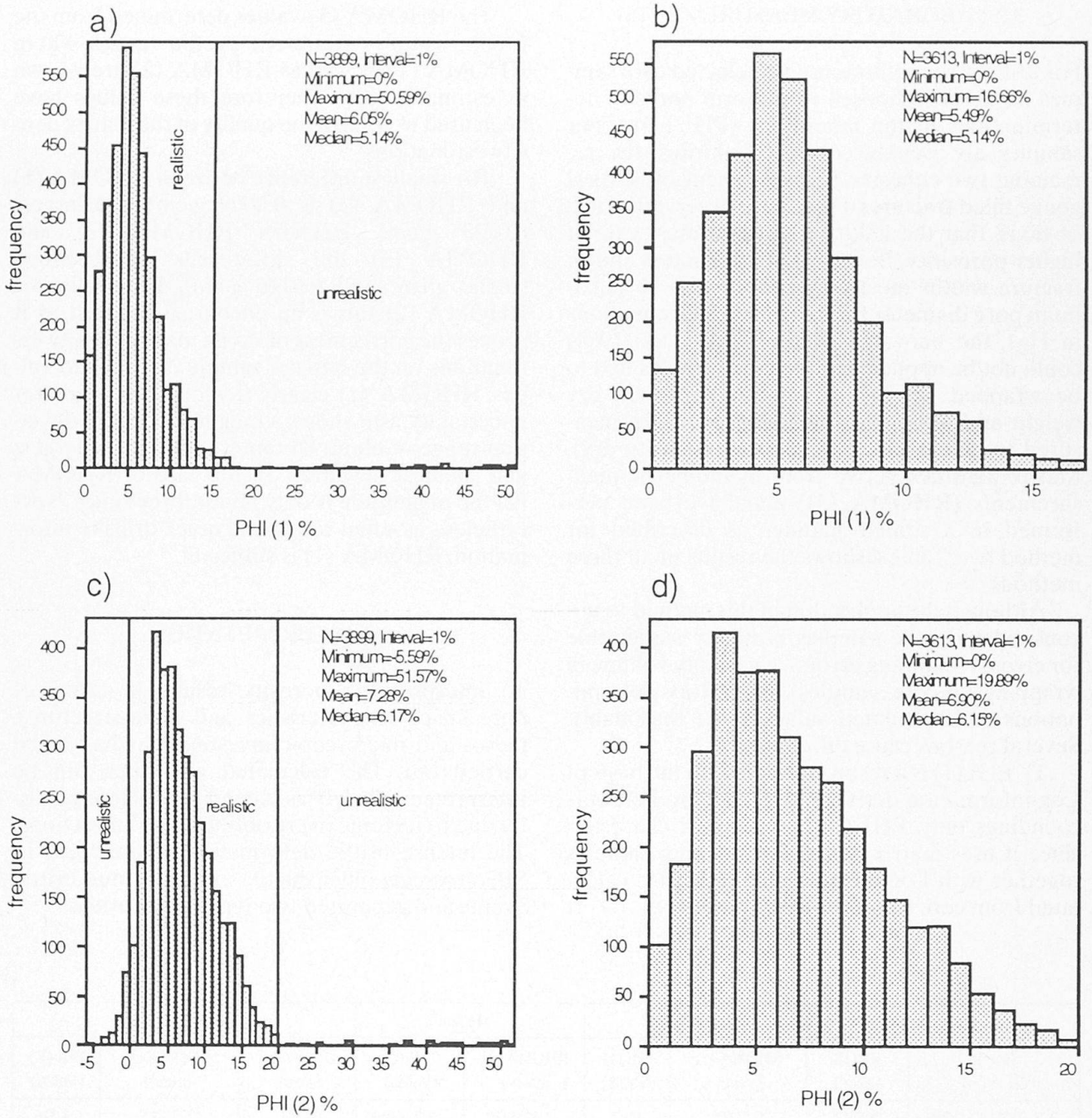

Fig. 4 *a)* Frequency distribution of PHI (1), including all values. Unrealistic values correspond to the cemented section. *b)* Frequency distribution of PHI (1), including realistic values only. The maximum frequency lies in the range 4–5% and the slope of the right shoulder is steep. *c)* Frequency distribution of PHI (2), including all values. Unrealistic values correspond to the cemented section. Negative unrealistic values correspond to the poor pyknometric measurement at 440 m, as well as to bad guesses in the assignment of RHOMA (2). *d)* Frequency distribution of PHI (2), including realistic values only. The maximum frequency lies in the range 3–4%. Compared to b), the maximum frequency is smaller, but the slope of the right shoulder is more gentle and goes to higher maximum values. This is due to the generally higher values of PHI (2) compared to PHI (1).

From frequency distribution evaluations (Fig. 4) it became evident that the maximum frequency of PHI (2) lies in a lower range (3–4%) than the maximum frequency of PHI (1) (4–5%). On the other hand, PHI (2) is generally higher than PHI (1).

3.2. LABORATORY MEASUREMENTS

For testing the methods used, 6 selected core samples have been choosen to perform porosity determinations in the laboratory (PHI (3)). Four samples are weakly cohesive kakirites, the remaining two cohesive rocks, crosscut by several gouge filled fractures. From core observation it is obvious, that the kakiritic samples must exhibit higher porosities. Because pore diameters and/or fracture widths mostly exceed 0.3 mm (= maximum pore diameter for buoyancy determinations in Hg), the buoyancy method (MÜLLER, 1964) could not be applied and the core samples had to be wrapped up. Instead of the buoyancy, dry weight and water displacement have been measured to determine rock densities (density dry). Matrix densities derive from pyknometric measurements (RHOMA (3)) and have been performed in a similar manner as described for method two. Table 4 shows the results of all three methods.

Although the application of this method to unconsolidated core samples is highly susceptible for errors ("handling errors", e.g. empty volume in wrapping up core samples), laboratory determinations and calculated values agree reasonably. Several reasons cause differences:

1) PHI (1) is a result calculated on the basis of Log-information deriving from the borehole surroundings only. PHI (2) has a mixed character, since it uses matrix densities from core samples together with Log-information. PHI (3) is calculated from core sample information only.

2) The depth location of the core samples cannot be identified precisely using the FMS-image. PHI (1) and PHI (2) in table 4 are mean values over the depth range of the samples.

3) During transport from borehole to laboratory the core samples suffered a lot of mechanical wear. Relaxation effects must be taken into account.

The RHOMA (3)-values determined from the 6 core samples represent profile ranges where RHOMA (1) as well as RHOMA (2) are known as estimates only. Therefore these values have been used to control the quality of the matrix density estimations.

The smallest difference between RHOMA (1) and RHOMA (3) is 0.0009 g/cm³, the largest 0.0773 g/cm³. Between RHOMA (2) and RHOMA (3) the differences lie between 0.0400 g/cm³ and 0.0126 g/cm³. Especially for RHOMA (2) this is an encouraging result as it proves the correctness of doing matrix density estimations on the basis of sample determined values. RHOMA (1) clearly demonstrate a greater uncertainty as it shows a magnitude in the deviation range of about 86 times between the largest and smallest deviation. In the case of RHOMA (2) the magnitude is only about three times. Nevertheless, as a first rough and quick drillsite information, RHOMA (1) is sufficient.

3.3. INTERPRETATION

To interpret the porosity results in terms of pore space characteristics and rock structures, meso- and microscopic investigations had to be carried out. The calculated porosities can be interpreted primarly as secondary fracture porosity due to tectonic overprinting (core inspection). The intense brittle deformation of the rocks in SB3 crosscuts older ductile and cemented brittle events and generated two types of kakirites.

		Method 1		Method 2		Laboratory check		
Sample depth (m)	RHOB (g/cm³)	RHOMA (1) (g/cm³)	PHI (1) (Vol.%)	RHOMA (2) (g/cm³)	PHI (2) (Vol.%)	Density dry (g/cm³)	RHOMA (3) (g/cm³)	PHI (3) (Vol.%)
320.93–321.29	2.583	2.742	9.41	2.8089	12.86	2.44	2.7715	11.96
323.38–323.64	2.592	2.742	8.84	2.8093	12.33	2.45	2.7693	11.53
348.48–348.64	2.777	2.812	2.00	2.7952	1.06	2.67	2.8111	5.02
420.44–420.55	2.733	2.781	2.77	2.7954	1.55	2.65	2.7560	3.85
442.25–442.55	2.668	2.790	6.99	2.7387	4.16	2.48	2.7127	8.58
520.46–520.75	2.644	2.694	3.07	2.7671	7.19	2.51	2.7545	8.88

Tab. 4 Correlation PHI (log) versus PHI (3). RHOB, RHOMA (1), RHOMA (2), PHI (1) and PHI (2) are mean values over the depth ranges of the core samples.

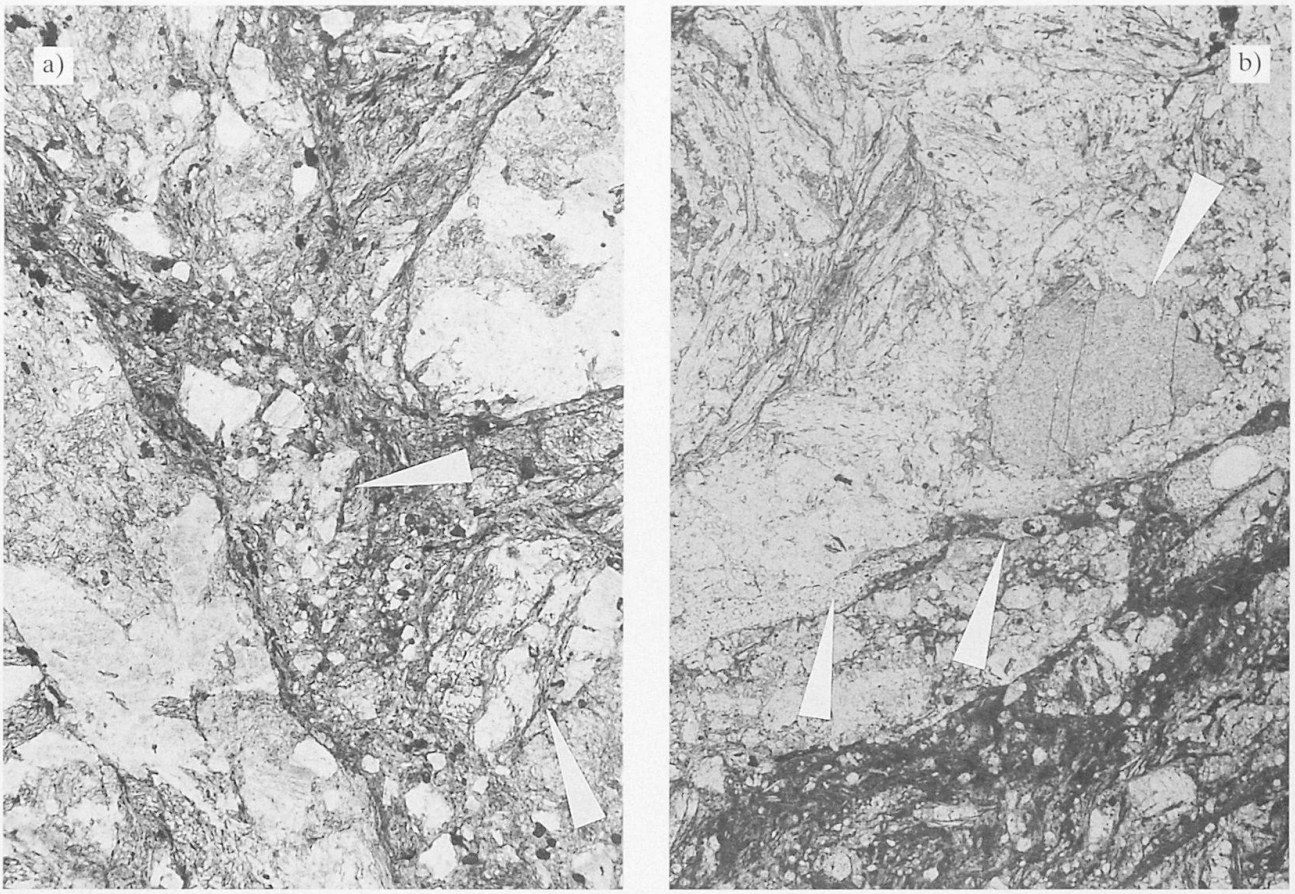

Fig. 5 (a) Kakirite, showing host rock clasts in cohesionless gouge (darker area) exhibiting microporosity. Upper arrow: broken quartz fragments. Lower arrow: fracture network within host rock clast. (b) Transition from highly fractured host rock (light area) into kakirite (darker area). The host rock is weakly cohesive only. Upper arrow: Calcite filled vug. Arrow is pointing to earlier grown hypidiomorphic quartz crystal. Lower arrows: incompletely filled fracture exhibiting fracture porosity. Picture widths 3.6 mm.

Most kakirites and soft rocks in SB3 belong to *type one* and still show the Alpine fabric but are crosscut by fracture networks parallel and discordant to the main schistosity. The thin sections show that most of the fractures are partly or completely filled with clayey cohesionless gouge generated by small displacement (mm-range) in combination with the formation of new sheet silicates along fracture planes.

In the less abundant *second type*, larger amounts of shear movement (cm-range) caused the total destruction of the Alpine fabric, leaving a matrix of cohesionless gouge that consists of fine grained detrital and newly grown sheet silicates and contains abraded rock and mineral clasts. Such zones of larger displacement are present mainly in depth ranges of 200 m – 300 m (no log reading from 0 m – 300 m), 300 m – 350 m and 600 m – 650 m. They occur in the range of some centimeters up to 1.2 meters.

On a mesoscopic scale it is easy to distinguish both types. But in thin sections, it is obvious that they mostly occur together on a small scale (Fig. 5). These structures exhibit impermeable intercrystalline microporosity within gouge between statistically or preferred oriented platy minerals. Preferred orientation of sheet silicates is associated with cataclastic flow features. The cohesionless and muddy behaviour of kakirites prevents the occurrence of continuous empty fractures. Single fractures rarely show lengths exceeding a few centimeters and therefore do not contribute to the permeability of the rocks.

Another contribution to the total porosity is the occurrence of vugs. Completely filled vugs may show growth of idiomorphic quartz crystals. Subsequent precipitation of calcite is filling the remaining interstices between the quartz crystals (Fig. 5). But in many cases the cementation by calcite is lacking and filling of the (not interconnected) vugs remains incomplete.

Combining and interpreting the meso- and microscopic observations from above, the permeability of the rocks in SB3 seems to be small. This

is also supported by the packer tests (see section 1.2). But it must be taken into account that some discrete kakiritic zones (in the range of centimeters to tens of meters) may locally possess significant permeabilities (incomplete or lacking filling of fractures) enabling water flow. Unfortunately, there is no mathematical relation between porosity and permeability. To draw quantitative conclusions about permeability from porosity values alone is not justified. The determination of permeabilities would need further work, including a complex interpretation of the seismic velocities. This is not within the scope of this study.

The mean porosities in the logged profile of 5.49% (PHI (1)) and 6.90% (PHI (2)) reveal that the porosity in the northern Tavetsch massif is generally significantly higher than in "normal" crystalline rocks. Kakirites will still be present at greater depths because there is no systematic decrease of porosity with depth in both profiles (Fig. 2).

For comparison: PRINZ (1991) gives values between 0.05% and 0.3% for granitic gneiss and hornblende gneiss. Porosities > 4% thus only occur as a result of surface processes like e.g. weathering.

4. Error analysis

4.1. ERROR PROPAGATION

Because absolute errors are unknown for the density log readings as well as for the pyknometric results, the mean error of the porosity determination is treated below. The analysis is based on the mean errors of the parameters involved. From Gaussian error propagation the mean error of porosity, ΔPHI is

$$\Delta\Phi = \pm\sqrt{\left(\frac{\partial\Phi}{\partial\rho_{ma}}\cdot\Delta\rho_{ma}\right)^2+\left(\frac{\partial\Phi}{\partial\rho_{fl}}\cdot\Delta\rho_{fl}\right)^2+\left(\frac{\partial\Phi}{\partial\rho_b}\cdot\Delta\rho_b\right)^2} \quad (4)$$

and by inserting the first derivatives Φ' to be derived from equ. (1):

$$\Delta\Phi = \pm\sqrt{\left(\frac{\rho_b-\rho_{fl}}{(\rho_{ma}-\rho_{fl})^2}\cdot\Delta\rho_{ma}\right)^2+\left(\frac{\rho_{ma}-\rho_b}{(\rho_{ma}-\rho_{fl})^2}\cdot\Delta\rho_{fl}\right)^2+\left(\frac{-1}{(\rho_{ma}-\rho_{fl})}\cdot\Delta\rho_b\right)^2} \quad (5)$$

Since $\rho_{ma} \geq \rho_b > \rho_{fl}$ it can be seen from equ. (5) that for the first derivatives

$$|\Phi'(\rho_b)| \geq |\Phi'(\rho_{ma})| > |\Phi'(\rho_{fl})|$$

Thus uncertainties in RHOB lead to the largest, in RHOFL to the smallest error (when keeping all other parameters and errors constant).

For a specific example with RHOMA = 2.8000 g/cm³, RHOFL = 1.1000 g/cm³ and RHOB = 2.7000 g/cm³ (equ. (1)) yields PHI = 13.73%. Assuming the same error (± 0.0100 g/cm³) for all densities, from equ. (5) follows

$$\Delta\Phi = \pm\sqrt{3.0651\cdot10^{-5}+1.1973\cdot10^{-7}+3.4460\cdot10^{-5}} = \pm 0.0081 \quad (6)$$

or $\Delta\Phi = \pm 5.89\%$ of Φ

thus $\Phi = (13.73 \pm 0.81)\ \%$.

Equ. (6) clearly demonstrates that uncertainties in RHOFL have practically no contribution to the error in porosity. Therefore for the following treatment ΔRHOFL = 0 can be assumed, and only the uncertainty in RHOMA and RHOB will be considered. Equ. (5) reduces to

$$\Delta\Phi = \pm\frac{1}{(\rho_{ma}-\rho_{fl})}\cdot\sqrt{\frac{(\rho_b-\rho_{fl})^2}{(\rho_{ma}-\rho_{fl})^2}\cdot\Delta\rho_{ma}^{\,2}+\Delta\rho_b^{\,2}} \quad (7)$$

4.2. MEAN ERROR OF RHOB AND RHOMA

The mean error of RHOB is, according to SCHLUMBERGER (personnel communication), ± 0.01 g/cm³. For a constant error of RHOB the porosity change remains constant (equ. (5)). Therefore the bulk density of a given rock has no influence on the porosity error caused by a RHOB uncertainty; the porosity error is relevant only for the ratio error/porosity value: the smaller the porosity, the larger the relative error.

As described in chapter 2.3.2, RHOMA (2) has been determined in the laboratory by the pyknometric method. In these determinations care was taken not to exceed a mean error of ± 0.01 g/cm³, in order to minimize the total error in porosity (Tab. 2). RHOMA was therefore determined for each sample at least three times or as often as needed to remain below the above mentioned error value. For the mean error of RHOMA the standard deviation of the mean was calculated for each sample.

For a constant error value of RHOMA small porosities have a larger uncertainty than large values. In other words: for high porosities RHOMA can be selected more deliberately in a wider interval than for small porosities (should the porosity error remain within a certain range). For large RHOB values the maximum slope of the function decreases. Thus the maximum error is smaller for high-density rocks than for low-density ones.

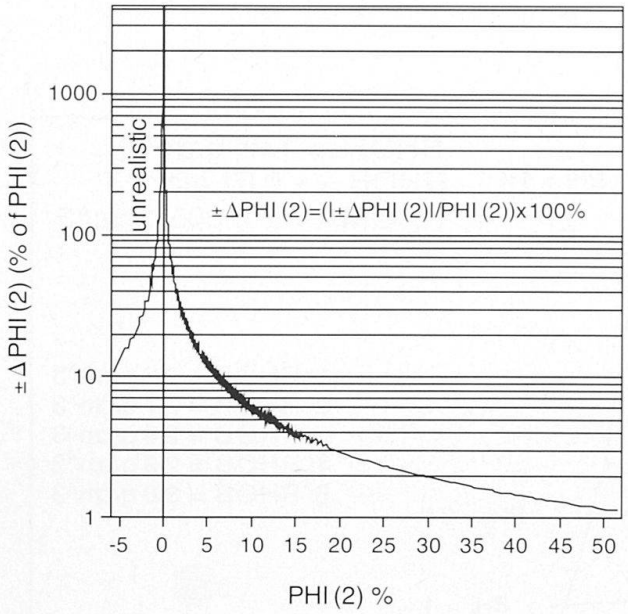

Fig. 6 Porosity-mean error crossplot of PHI (2). Note the strong increase of the mean error with decreasing PHI (2).

4.3. RESULTS OF THE ERROR CALCULATION

In the appendix "Por Listing" the results of the error calculation are given as relative error (percent value of PHI (2) in the column ± ΔPHI (2)). The mean errors of RHOMA (2) are given in g/cm³ in the column ± ΔRHOMA (2).

Figure 6 shows a clear trend: the smaller the porosity value the larger the mean error.

For porosity values > 3% the mean relative error lies below 20% and is still acceptable. The error increases for small porosities. Generally the relation between porosity and mean error can be described with the following equation:

$$n = \frac{|\Delta\Phi|}{\Phi} \qquad (8)$$

n is the absolute value of the relative error and thus

$$n \geq 0.$$

This equation can be solved for the error parameters ± ΔRHOMA, ± ΔRHOB and ± ΔRHOFL, taking into account equ. (5). If for example ± ΔRHOB and ± ΔRHOFL are known and the error value should be < 20% it is possible to solve equ. (8) for ± ΔRHOMA. The needed accuracy of the matrix density can then be calculated. If ± ΔRHOB and ± ΔRHOFL already cause an error > 20% the equation gives no solution and the calculation of porosity values within the demanded error range is not possible.

In order to obtain a value smaller than 10%, ΔRHOB must be smaller than ± 0.01 g/cm³. This would need higher count rates and thus more sensitive detectors in the logging tool, even for low logging speeds.

4.4. DERIVATION OF PHI-ERROR-CHARTS

Equ. (8) can be written as a function of RHOMA:

$$n(\rho_{ma}) = \frac{1}{\rho_{ma} - \rho_b} \cdot \left| \pm \sqrt{(\rho_b - \rho_{fl})^2 \cdot \Delta\rho_{ma}^2 + \Delta\rho_b^2} \right| \qquad (9)$$

with

$$n > 0.$$

Now n can be plotted against RHOMA, with ΔRHOB, ΔRHOMA and RHOFL = constant for different values of RHOB (Fig. 7). In general ΔRHOB, and RHOFL are known. In case of ΔRHOMA one can choose a value that is certainly reachable with pyknometric measurements. As in this study ΔRHOMA was always smaller than ± 0.0073 g/cm³, a value of ± 0.0050 g/cm³ has been choosen for figure 7. ΔRHOB was taken as ± 0.01 g/cm³, the value given by SCHLUMBERGER (personnel communication). The aim of the chart is to decide, if for a given RHOB a reasonable porosity value can be determined. Knowing the lithology, an estimation for RHOMA can be done. With this value one can enter the chart and read the porosity and the error value (n) from the curve corresponding to the given value of RHOB (log reading). The chart offers the possibility to decide quickly if porosity calculations are adequate. It should be a tool for the drillsite geologist in the same manner as the "Log Interpretation Charts" available from SCHLUMBERGER (1991). Figure 6 can be drawn for any combination of values for the constant parameters.

5. Discussion

The close correlation between the results of the two methods has shown that acceptable results can be obtained by both methods. 52 of 57 (or 91.2 %) of the error values of PHI (2) calculated from their sample matrix density are below 20% of their porosity values. In addition, the corresponding ratios RHOMA (1) / RHOMA (2) are mainly close to 1 (Tab. 2). The ratio RHOMA (1) / RHOMA (2) shows the quality of the estimation of RHOMA (1). A successful estimation of RHOMA (1) yields a ratio close to 1.00. From this it follows that by having a good knowledge of

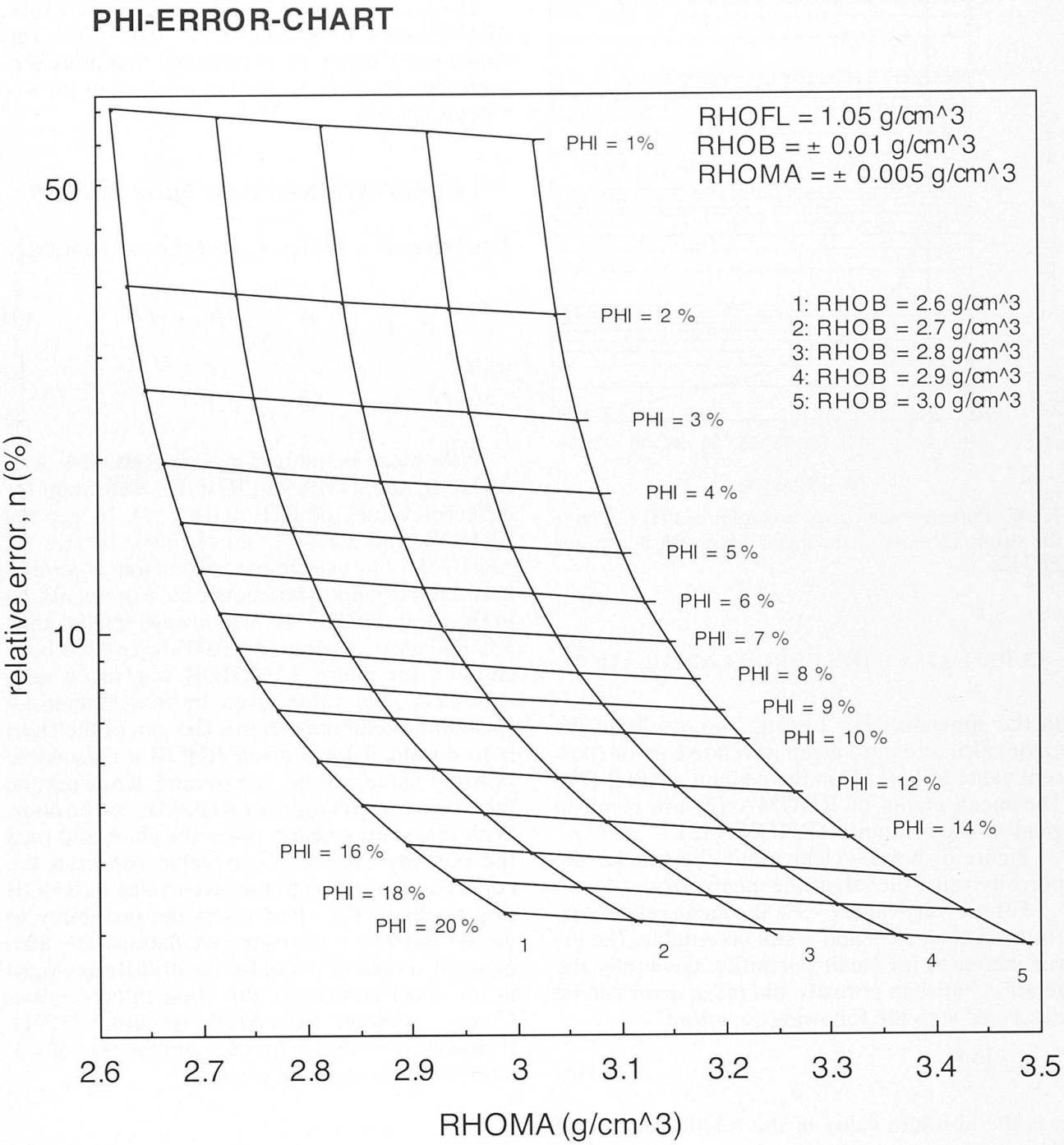

Fig. 7 Mean error curves against RHOMA for different values of RHOB. Interceptions are lines of constant porosity. Further explanations see text.

the borehole lithology, complemented by an accurate interpretation of the lithology-sensitive logging traces, it is possible to estimate reasonable values for RHOMA (1) and to calculate continuous porosity profiles. For a first rough porosity information the first method is useful. The second method is more accurate as it includes measurements of matrix densities and takes mean errors into consideration. Combining both methods gives additional security for reliable results.

The mathematical error treatment (chapter 4) reveals the difficulty in determining small porosity values. To reduce the error of small values, $\pm$ ΔRHOB must be distinctly smaller than 0.01 g/cm^3. The value of $\pm$ ΔRHOMA can be held very small by performing pyknometric measurements. Therefore the limitations of the presented

methods for determining porosity lie in the experimental configuration of the logging tool. As long as the accuracy of the tool is ± 0.01 g/cm³, the lower limit of determining porosity within a relative error of ± 20% lies around 3% (Fig. 6).

Along the profile PHI (2), 268 of 3899 (or 6.9%) of all porosity values are unrealistic (including the 158 values or 4.1% in the cemented part). Because of the pyknometric measurements, the values of PHI (2) are more realistic than those of PHI (1).

Subtracting the values in the cemented part of the borehole from the unrealistic values of PHI (2), the remaining 2.8% reflect the geological and experimental errors of the worker doing porosity determination.

Thin section studies on rock structures revealed that the actual porosity of the rocks in SB3 is a result of intense brittle deformation (Fig. 5). The syn- to post-deformational precipitation of new minerals (mainly sheet silicates) calls for an impermeable microporosity within fractures and vugs. The loss of rock cohesion in kakirites is induced by increasing density of fracture networks (and therefore of total porosity) crosscutting older structures.

6. Conclusions

1) A good knowledge of the lithology, complemented by log interpretations allow to derive reasonable porosities from density logs. The procedures presented require the knowledge of the local rocks, they should be applied in close cooperation with the drillsite geologist. Applying and correlating both methods of porosity determination (1: matrix density estimation from maximum log readings, 2: pyknometric matrix density determinations) allows to judge the quality of the results. They may be classified as realistic or unrealistic. This classification compensates for a certain degree the lack of knowing the absolute errors.

2) Six checks by laboratory determinations show reasonable agreement.

3) By error analysis it can be demonstrated that for high-density rocks porosity determination is more accurate than for low-density ones. Applying the methods presented for crystalline rocks, high-density rocks like crystalline ore formations, basaltic rocks, metabasites, mantle derived rocks and meta-ultrabasites will yield the best results concerning mean errors.

4) Small porosity values are very difficult to determine. The reason that the quality of the presented porosity profiles is rather high lies in the fact that the porosity in the Tavetsch massif is generally high. In a massive, tectonically undisturbed granite body with porosities much smaller than 3%, the entire procedure would have been questionable.

5) The mean errors of porosity are strongly dependent on ± ΔRHOB. The limitations of the presented methods is dictated by the technical equipment. The mean error of matrix densities can be held very small, and the mean error of the fluid density is negligible.

6) A comparison of mean porosities in 50 m intervals with corresponding amounts of kakiritic rocks deduced in the "rock statistics" (SCHNEIDER, 1993) fits well. Small scale correlations between porosity peaks and discrete kakirite zones also show good coincidences.

7) The northern Tavetsch massif is highly porous, at least in the investigated area. At the same time permeability is small. The lack of a systematic decrease of porosity with depth indicates deep reaching brittle destruction of the rocks and an increase of their volume (dilatancy). It is probable that a large percentage of the investigated rocks in drillhole SB3 are possibly still desaggregated and cohesionless down to the depth range of the projected Gotthard base tunnel.

Acknowledgements

This study was performed within the framework of the Ph. D. Thesis by R.F.W. under the advice of M. Frey, S. Schmid and L. Hauber (University of Basel). R.F.W. thanks his advisers for the financial and logistic support during the course of this study.

R.F.W. is grateful to G. Sattel (Ingenieurbüro Amberg AG, Regensdorf/ZH) for introducing him into the art of log interpretation. G. Sattel made available the logging data from SB3-Tujetsch. During many discussions, C. Schindler (ETHZ) convinced us about the necessity of this work. We also thank the company of Schlumberger (Hannover/D) for the pleasant cooperation.

J. Blickenstorfer (Projektleitung Alp Transit Gotthard, SBB) made available the samples for matrix density determinations.

Finally, we thank R. Gieré (University of Basel) for his careful rewiew of the first manuscript and M. Kirschen (University of Basel) for helpful discussions and suggestions. The final version benefitted from constructive rewiews by G. Sprecher, P. Blümling, S. Vomvoris (Nagra, Wettingen) and Ch. Bücker (Aachen).

References

BROGLIA, C. and MOOS, D. (1988): In-situ structure and properties of 110 Ma crust from geophysical logs in DSDP hole 418A. Proceedings of the Ocean Drilling Program, Scientific Results 102, 29–47.

DESBRANDES, R. (1985): Encyclopedia of well logging. Editions Technip, Paris, 584 pp.

ELLIS, D.V. (1987): Well logging for earth scientists. Elsevier Science Publishers, Amsterdam, 532 pp.

HEITZMANN, P. (1985): Kakirite, Kataklasite, Mylonite – Zur Nomenklatur der Metamorphite mit Verformungsgefügen. Eclogae geol. Helv., Vol. 78, 273–286.

MÜLLER, G.M. (1964): Methoden der Sedimentuntersuchung. E. Schweizerbart'sche Verlagsbuchhandlung (Nägele und Obermiller), Stuttgart, 303 pp.

NELSON, P.H. and JOHNSTON, D. (1994): Geophysical and geochemical logs from a copper oxide deposit, Santa Cruz project, Casa Grande, Arizona. Geophysics 59, 1827–1838.

NIGGLI, E. (1944): Das westliche Tavetscher Zwischenmassiv und der angrenzende Nordrand des Gotthardmassivs. Petrographisch-geologische Untersuchungen. Diss. Universität Zürich.

PRINZ, H. (1991): Abriss der Ingenieurgeologie. Ferdinand Enke Verlag, Stuttgart, 2. Auflage, 466 pp.

SCHLUMBERGER (1991): Log interpretation charts. Schlumberger educational services.

SCHNEIDER, T.R. (1991): Auswertung der Sondierungen Tujetsch 1991, Schlussbericht. Alp Transit, Achse Gotthard, Bericht Nr. 425 ah.

SCHNEIDER, T.R. (1994): Auswertung der Sondierung Tujetsch 1993, SB3. Alp Transit, Achse Gotthard, Bericht Nr. 425bj.

SERRA, O. (1984): Fundamentals of well-log interpretation. Vol. 1: The acquisition of logging data. Elsevier Science Publishers. Developments in Petroleum Science 15A, Amsterdam, 423 pp.

TITTMAN, J. (1986): Geophysical Well Logging. Academic Press, New York, 175 pp.

ZIMMERMANN, G., BURKHARDT, H. and MELCHERT, M. (1992): Estimation of porosity in crystalline rock by a multivariate statistical approach. Scientific Drilling 3, 27–35.

Manuscript received November 6, 1995; revision accepted April 30, 1996.

Appendix

Description of the table "Por Listing"

Remark:

The columnns "Tiefe" and "RHOB" are log-read values, extracted from the original logging data file "COMPOSITE LOG SB3.ED.XLS". The data set has been made available by Dr. G. Sattel, AMBERG INGENIEURBÜRO AG (Regensdorf/ZH) who did the geophysical interpretation of the composite log (SCHNEIDER, 1994: Beilage 425bj/7, Sondierung Tujetsch 1993, Geophysikalische Messungen in der Bohrung SB3).

Main elements:

1) The column "ZONENNR." indicates the zone for RHOMA (1).
2) Bold printed lines mark sample positions of RHOMA (2).

Columns:

Tiefe:	position of log measurement
RHOB:	bulk density read from log
± ΔRHOB:	mean error of RHOB
RHOFL:	density of drilling mud. The fluid in the zone investigated by the logging tool is mainly drilling mud displacing the natural pore filling.
RHOMA (1):	estimated matrix density
ZONENNR.:	zone division for the estimation and distribution of RHOMA (1)
PHI (1):	total porosity calculated with: RHOB, RHOFL, RHOMA (1)
RHOMA (2):	**bold print:** pyknometric measurement of matrix density normal print: pyknometric measurement distributed as estimation
± ΔRHOMA (2):	mean error of pyknometric measurement of RHOMA (2)
PHI (2):	total porosity calculated with: RHOB, RHOFL, RHOMA (2)
± ΔPHI (2):	mean error of PHI (2) calculated with: ± ΔRHOB, ± ΔRHOMA (2)
PHI (1) / PHI (2) and RHOMA (1)/ RHOMA (2):	ratio of porosities and matrix densities. The closer the value lies to 1 the better the coincidence between both methods of porosity estimation. Very good values give 1.00 (rounded to the second decimal point). The quality of coincidence between both methods **is independent of ± ΔPHI (2)**.

Bemerkung zu PHI (2):

Messung (bold):	RHOMA (2) determined by pyknometry. The result PHI (2) is calculated with measured parameters only.
Schätzung:	RHOMA (2) determined by pyknometry used as estimation value.
Unrealistisch:	PHI (2) < 0%, result unrealistic.
Grey colour:	cemented borehole section from 556 m to 580 m. PHI (2) **and** PHI (1) unrealistic (158 values).
50 m Mittel realistisch:	mean of PHI (2) within 50 m intervals according to the intervals used in the "drill statistics". Only realistic values used.

Note: As the whole table "Por Listing" contains 79 pages, only one page is given here as an example. The whole data set is available from the first author.

Tab. A1: "Por Listing"

Tiefe	RHOB	± ΔRHOB	RHOFL	RHOMA (1)	ZONEN-NR.	PHI (1)	RHOMA (2)	± RHOMA (2)	PHI (2)	± PHI (2)	PHI (1)/ PHI (2)	RHOMA (1)/ RHOMA (2)	Bemerkung	50m Mittel
m	g/cm³	g/cm³	g/cm³	g/cm³		Vol.%	g/cm³	g/cm³	Vol.%	%Eigenwert			zu PHI (2)	realistisch
549.86	2.680	0.01	1.03	2.730	18	2.94	2.7645	0.0017	4.87	11.99	0.60	0.99	Schätzung	
550.01	2.690	0.01	1.03	2.730	18	2.35	2.7645	0.0017	4.30	13.60	0.55	0.99	Schätzung	8.94
550.16	2.650	0.01	1.03	2.730	18	4.71	2.7645	0.0017	6.60	8.84	0.71	0.99	Schätzung	
550.32	2.630	0.01	1.03	2.730	18	5.88	2.7645	0.0017	7.75	7.53	0.76	0.99	Schätzung	
550.47	2.600	0.01	1.03	2.730	18	7.65	2.7645	0.0017	9.48	6.15	0.81	0.99	Schätzung	
550.62	2.610	0.01	1.03	2.730	18	7.06	2.7645	0.0017	8.91	6.55	0.79	0.99	Schätzung	
550.77	2.620	0.01	1.03	2.730	18	6.47	2.7645	0.0017	8.33	7.00	0.78	0.99	Schätzung	
550.93	2.640	0.01	1.03	2.730	18	5.29	2.7645	0.0017	7.18	8.13	0.74	0.99	Schätzung	
551.08	2.660	0.01	1.03	2.730	18	4.12	2.7645	0.0017	6.02	9.69	0.68	0.99	Schätzung	
551.23	2.660	0.01	1.03	2.730	18	4.12	2.7645	0.0017	6.02	9.69	0.68	0.99	Schätzung	
551.38	2.650	0.01	1.03	2.730	18	4.71	2.7645	0.0017	6.60	8.84	0.71	0.99	Schätzung	
551 54	2.640	0.01	1.03	2.730	18	5.29	2.7645	0.0017	7.18	8.13	0.74	0.99	Schätzung	
551.69	2.650	0.01	1.03	2.730	18	4.71	2.7645	0.0017	6.60	8.84	0.71	0.99	Schätzung	
551.84	2.620	0.01	1.03	2.730	18	6.47	2.7645	0.0017	8.33	7.00	0.78	0.99	Schätzung	
551.99	2.580	0.01	1.03	2.730	18	8.82	2.7645	0.0017	10.64	5.48	0.83	0.99	Schätzung	
552.15	2.600	0.01	1.03	2.730	18	7.65	2.7645	0.0017	9.48	6.15	0.81	0.99	Schätzung	
552.30	2.630	0.01	1.03	2.730	18	5.88	2.7645	0.0017	7.75	7.53	0.76	0.99	Schätzung	
552.45	2.730	0.01	1.03	2.730	18	0.00	2.7645	0.0017	1.99	29.39	0.00	0.99	Schätzung	
552.60	2.660	0.01	1.03	2.730	18	4.12	2.7645	0.0017	6.02	9.69	0.68	0.99	Schätzung	
552.76	2.660	0.01	1.03	2.730	18	4.12	2.7645	0.0017	6.02	9.69	0.68	0.99	Schätzung	
552.91	2.620	0.01	1.03	2.730	18	6.47	2.7645	0.0017	8.33	7.00	0.78	0.99	Schätzung	
553.06	**2.650**	**0.01**	**1.03**	**2.730**	**18**	**4.71**	**2.7645**	**0.0017**	**6.60**	**8.84**	**0.71**	**0.99**	**Messung**	
553.21	2.650	0.01	1.03	2.730	18	4.71	2.7645	0.0017	6.60	8.84	0.71	0.99	Schätzung	
553.36	2.660	0.01	1.03	2.730	18	4.12	2.7645	0.0017	6.02	9.69	0.68	0.99	Schätzung	
553.52	2.670	0.01	1.03	2.730	18	3.53	2.7645	0.0017	5.45	10.72	0.65	0.99	Schätzung	
553.67	2.660	0.01	1.03	2.730	18	4.12	2.7645	0.0017	6.02	9.69	0.68	0.99	Schätzung	
553.82	2.670	0.01	1.03	2.730	18	3.53	2.7645	0.0017	5.45	10.72	0.65	0.99	Schätzung	
553.97	2.650	0.01	1.03	2.730	18	4.71	2.7645	0.0017	6.60	8.84	0.71	0.99	Schätzung	
554.13	2.650	0.01	1.03	2.730	18	4.71	2.7645	0.0017	6.60	8.84	0.71	0.99	Schätzung	
554.28	2.620	0.01	1.03	2.730	18	6.47	2.7645	0.0017	8.33	7.00	0.78	0.99	Schätzung	
554.43	2.620	0.01	1.03	2.730	18	6.47	2.7645	0.0017	8.33	7.00	0.78	0.99	Schätzung	
554.58	2.610	0.01	1.03	2.730	18	7.06	2.7645	0.0017	8.91	6.55	0.79	0.99	Schätzung	
554.74	2.590	0.01	1.03	2.730	18	8.24	2.7645	0.0017	10.06	5.80	0.82	0.99	Schätzung	
554.89	2.560	0.01	1.03	2.730	18	10.00	2.7645	0.0017	11.79	4.94	0.85	0.99	Schätzung	
555.04	2.570	0.01	1.03	2.730	18	9.41	2.7399	0.0045	9.94	6.35	0.95	1.00	Schätzung	
555.19	2.550	0.01	1.03	2.730	18	10.59	2.7399	0.0045	11.11	5.67	0.95	1.00	Schätzung	
555.35	2.560	0.01	1.03	2.730	18	10.00	2.7399	0.0045	10.52	5.99	0.95	1.00	Schätzung	
555.50	2.540	0.01	1.03	2.730	18	11.18	2.7399	0.0045	11.69	5.38	0.96	1.00	Schätzung	
555.65	2.570	0.01	1.03	2.730	18	9.41	2.7399	0.0045	9.94	6.35	0.95	1.00	Schätzung	
555.80	2.600	0.01	1.03	2.730	18	7.65	2.7399	0 0045	8.18	7.73	0.93	1.00	Schätzung	
555.96	2.620	0.01	1.03	2.730	18	6.47	2.7399	0.0045	7.01	9.04	0.92	1.00	unrealistisch	
556.11	2.610	0.01	1.03	2.730	18	7.06	2.7399	0.0045	7.60	8.34	0.93	1.00	unrealistisch	
556.26	2.620	0.01	1.03	2.730	18	6.47	2.7399	0.0045	7.01	9.04	0.92	1.00	unrealistisch	
556.41	2.630	0.01	1.03	2.730	18	5.88	2.7399	0.0045	6.43	9.87	0.92	1.00	unrealistisch	
556.57	2.640	0.01	1.03	2.730	18	5.29	2.7399	0.0045	5.84	10.87	0.91	1.00	unrealistisch	
556.72	2.630	0.01	1.03	2.730	18	5.88	2.7399	0.0045	6.43	9.87	0.92	1.00	unrealistisch	
556.87	2.600	0.01	1.03	2.730	18	7.65	2.7399	0.0045	8.18	7.73	0.93	1.00	unrealistisch	
557.02	2.620	0.01	1.03	2.730	18	6.47	2.7399	0.0045	7.01	9.04	0.92	1.00	unrealistisch	
557.17	2.630	0.01	1.03	2.730	18	5.88	2.7645	0.0017	7.75	7.53	0.76	0.99	unrealistisch	
557.33	2.660	0.01	1.03	2.730	18	4.12	2.7645	0.0017	6.02	9.69	0.68	0.99	unrealistisch	